Journal of Power Sources 257 (2014) 213–220

Contents lists available at ScienceDirect

Journal of Power Sources

journal homepage: www.elsevier.com/locate/jpowsour

In situ synthesis of cobalt stabilized on macroscopic biopolymer hydrogel as economical and recyclable catalyst for hydrogen generation from sodium borohydride hydrolysis

Lunhong Ai, Xiaoyan Gao, Jing Jiang*

Chemical Synthesis and Pollution Control Key Laboratory of Sichuan Province, College of Chemistry and Chemical Engineering, China West Normal University, Nanchong 637002, PR China

HIGHLIGHTS

- Fabrication of biopolymer hydrogel stabilized cobalt catalyst was described.
- The Co@AHs catalyst exhibited high performance in the hydrolysis of $NaBH_4$.
- The Co@AHs catalyst can be easily separated and readily reused for catalytic application.

ARTICLE INFO

Article history:
Received 16 August 2013
Received in revised form
28 January 2014
Accepted 31 January 2014
Available online 11 February 2014

Keywords:
Hydrogen generation
Sodium borohydride
Hydrolysis
Cobalt
Biopolymer

ABSTRACT

In this study, we describe the successful fabrication of cobalt grown *in situ* on macroscopic alginate hydrogels (Co@AHs) and demonstrate that the as-prepared Co@AHs can act as a cost-effective and recyclable catalyst for hydrogen generation from the hydrolysis of $NaBH_4$. The structure and morphology of the Co@AHs catalyst are identified by X-ray diffraction (XRD), Fourier transform infrared spectroscopy (FTIR), scanning electron microscopy (SEM), energy-dispersive spectroscopy (EDS), and X-ray photoelectron spectroscopy (XPS). The resultant Co@AHs samples show an excellent catalytic performance for the hydrogen generation from $NaBH_4$ hydrolysis. The catalytic activity of the Co@AHs towards the hydrolysis reaction is systematically investigated by varying different reaction parameters, such as the catalyst dosage, temperature, and initial concentration of $NaBH_4$ or NaOH. The Co@AHs catalyst can be easily separated after catalytic reaction and readily recycled over four successive reaction cycles. Considering that the eco-friendly and inexpensive Co@AHs is catalytically effective with superior recyclability, it should have potential application in the hydrogen generation from the hydrolysis of borohydrides.

1. Introduction

Growing global environmental concerns associated with excessive fossil fuels usage, coupled with the ever-increasing energy demands, have currently stimulated a broad, intensive search for alternative energy sources [1,2]. Hydrogen is one of the most attractive energy carriers because of its high gravimetric energy density, ideal combustion efficiency and non-toxicity. Unfortunately, the widespread hydrogen applications are limited greatly by the technological barriers of the hydrogen storage and delivery, attributing to its gaseous nature and low density at room temperature [3,4]. To this end, solid hydrogen storage materials with high capacity and safety have attracted intense attention. Among these, sodium borohydride ($NaBH_4$) has been identified as a good candidate for hydrogen storage owing to its high hydrogen content (10.8 wt%), high volumetric hydrogen density (113 kg m^{-3} H_2), low costs, potentially safe operation, as well as high stability under ambient conditions [5,6]. Notably, hydrogen generation reaction rate upon $NaBH_4$ hydrolysis is quite low, although this reaction is spontaneous at room temperature, but it can be accelerated in the presence of suitable catalysts. Therefore, it is desirable to explore novel catalysts with high efficiency for hydrogen generation.

As widely accepted, noble metals possess excellent catalytic activity towards the hydrogen generation, but their practical applications are restricted by the inevitable disadvantages of high

* Corresponding author. Tel.: +86 817 2568081; fax: +86 817 2582029.
E-mail address: 0826zjjh@163.com (J. Jiang).

http://dx.doi.org/10.1016/j.jpowsour.2014.01.119
0378-7753/

price and limited abundance. Recently, cost-effective non-noble metals, such as cobalt, nickel, and iron, have been developed as an alternative to noble metal catalysts. Unfortunately, the catalytic activity of non-noble metals is still not satisfactory. Particularly, they often suffer from undesirable durability due to the easy agglomeration stemming from the high surface-to-volume ratio and intrinsically magnetic interaction. To solve this problem, various solid supports including carbon [7–9], silica [10,11], zeolite [12], metal oxides [13,14], and synthetic hydrogels [15,16], have been employed to immobilize the non-noble metal catalysts to protect them against dissolution and aggregation. Recently, natural polysaccharide hydrogels have emerged as a new class of ideal active supporter for the immobilization of metallic nanoparticles, which have the advantages of biocompatibility, environmental sustainability, chemical tunability, and anticipated low cost. Their opened porous structure provides multiple accessible channels for the diffusion and transport of ions and molecules, which is attractive for practical applications. Besides, such type of hydrogels generally contains various functional groups, such as −COOH, −NH_2, and −OH, ensuring the interaction between metallic nanoparticles and polymer chains. In our previous work, we have demonstrated that the macroscopic biopolymer alginate hydrogels (AHs) can be directly used as a green and effective carrier to stabilize metal nanoparticles, achieving the excellent activity and durability for the catalytic reduction [17,18]. Thus, it is reasonably expected that alginate would be an effective polysaccharide biopolymer carrier for loading metallic cobalt to create high performance catalysts for hydrogen generation.

In the present study, we report a facile and scalable route to prepare new designed, catalytically active metallic cobalt *in situ* grown on macroscopic alginate hydrogels (Co@AHs) for the first time. The resultant Co@AHs catalysts show an excellent catalytic performance for the hydrogen generation from $NaBH_4$ hydrolysis. More interestingly, the Co@AHs catalyst can be easily separated after catalytic reaction and readily recycled over four successive reaction cycles. Since the eco-friendly and inexpensive Co@AHs is catalytically effective with superior recyclability, it should have potential application in the hydrogen generation from the hydrolysis of borohydrides.

2. Experimental

2.1. Materials

Cobalt nitrate ($Co(NO_3)_2\cdot 6H_2O$), sodium borohydride ($NaBH_4$), sodium alginate, calcium chloride ($CaCl_2$), and sodium hydroxide (NaOH) were purchased from Kelong Chemical Reagents Company (Chengdu, China) and used without further purification. All chemicals used in this study were of commercially available analytical grade.

2.2. In situ fabrication of Co@AHs catalysts

Co@AHs catalysts were synthesized *in situ* by a chemical reduction process using $NaBH_4$ in aqueous solution. A schematic diagram of the synthesis procedure is presented in Fig. 1. Typically, 1.5 g of sodium alginate powder was dissolved in 100 mL of deionized water at room temperature for 30 min to obtain a transparent and viscous solution. This solution was then slowly added drop by drop to an aqueous solution containing 2 wt% $CaCl_2$ and $Co(NO_3)_2\cdot 6H_2O$ using a syringe. The formed light red gel beads (in the web version) were kept in solution for 1 h, separated from the solution, and washed by deionized water. The gel beads were then rapidly dropped into a $NaBH_4$ solution to obtain Co@AHs and then used as the catalyst for hydrolysis of $NaBH_4$.

2.3. Characterization

The powder X-ray diffraction (PXRD) measurements were recorded on a Rigaku Dmax/Ultima IV diffractometer with monochromatized Cu Kα radiation ($\lambda = 0.15418$ nm). The Fourier transform infrared (FTIR) spectroscopy was measured on a Nicolet 6700 FTIR Spectrometric Analyzer using KBr pellets. The morphology was observed with a JEOL JSM-6510LV scanning electron microscope (SEM). The elemental composition of the samples was characterized by energy-dispersive X-ray spectroscopy (EDS, Oxford instruments X-Max). X-ray photoelectron spectroscopy (XPS) measurements were recorded on a Perkin–Elmer PHI 5000C spectrometer using monochromatized Al Kα excitation. All binding energies were calibrated by using the contaminant carbon ($C_{1S} = 284.6$ eV) as a reference.

2.4. Hydrogen generation measurement

The hydrogen generation experiments were performed by using classic water-displacement method. An alkaline-stabilized solution of $NaBH_4$ (10 mL, 5 wt%) was prepared by the addition of NaOH (5 wt%) in a flask for catalytic activity tests. The flask was immersed in thermostatic water bath to maintain at a given temperature. During the catalytic process, no stirring was adopted due to the presence of vigorous bubble induced by the generated hydrogen, facilitating the contact between the reactant and the catalyst. Different experimental parameters such as catalyst dosage, concentrations of NaOH or $NaBH_4$, and temperature were varied for the

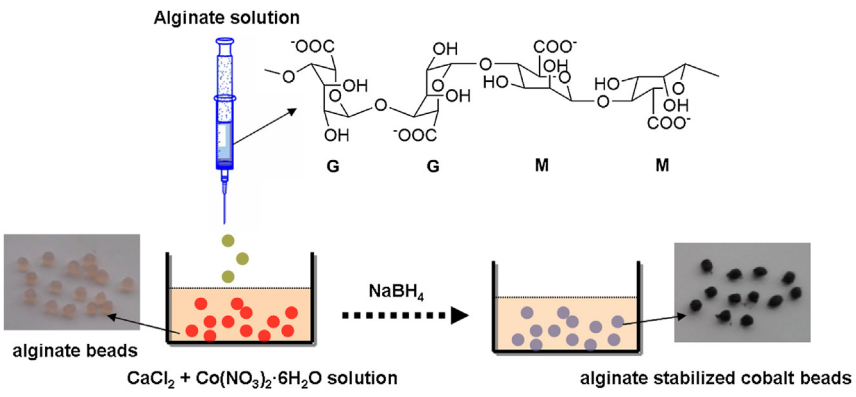

Fig. 1. Schematic illustration for the fabrication of the Co@AHs.

detailed study on $NaBH_4$ hydrolysis catalyzed by the Co@AHs. The activation energy was determined by test of hydrogen generation rates at different temperatures. For recyclability tests, the hydrolysis reactions were repeated four times. The first run refers to the *in situ* reduction and simultaneous $NaBH_4$ hydrolysis reaction. For the second to fourth run, the experiments were carried out in an equivalent volume (10 mL) of 5 wt% $NaBH_4$ solution containing 5 wt % NaOH.

3. Results and discussion

Alginate is an unbranched binary copolymer of 1,4-linked β-D-mannuronic acid and α-L-guluronic acid (Fig. 1), which is capable of forming hydrogels by cross-linking with a variety of divalent metal ions, such as calcium, barium, and cobalt. Interestingly, the as-formed three-dimensional network structure can serve as an ideal scaffold to support various functional materials for the wide applications. Inspired by these characteristics of alginate, we thereby propose the synthesis procedure to construct the Co@AHs catalysts, as schematically illustrated in Fig. 1. Using Ca^{2+} and Co^{2+} ions as cross-linkers, we first fabricate a heterogeneous bimetallic Ca^{2+}/Co^{2+}-alginate hydrogel beads. The supported Co^{2+} can then easily be reduced into metallic cobalt by simple treatment with $NaBH_4$, while the left Ca^{2+} as a strong cross-linker could maintain the structural stability of hydrogel beads, due to the lower reduction potentials of Ca(II)/Ca(0) (reduction potentials: E^0 Ca(II)/Ca(0) = −2.868 eV vs. SHE; E^0 Co(II)/Co(0) = −0.28 eV vs. SHE).

Fig. 2a shows the typical X-ray diffraction (XRD) patterns of the Co@AHs. Clearly, sodium alginate presents typical characteristic peaks at 14.3°, 21.6° and 36.7°, which are similar to those reported in the literature [19,20]. The XRD pattern of Co@AHs demonstrates the amorphous structure of the sample. The basic diffraction peaks are observed in the 2θ range of 15–40°, which are similar to those reported for the alginate beads [19,21]. Notably, it can be seen the decrease in the intensity of these diffraction peaks and the disappearance of the peak at 14.3°, because the reduction of the cobalt species has created more disorder in the system. Furthermore, the molecular structure and functional groups of the Co@AHs were confirmed by Fourier transform infrared (FTIR) spectroscopy, as shown in Fig. 2b. For Ca^{2+}/Co^{2+}-AHs, the intense band at 3440 cm^{-1} is assigned to the stretching of O–H. The band at 2924 cm^{-1} is associated with the C–H stretching of methyne groups. The bands at 1097 and 1037 cm^{-1} are attributed to the stretching of C–O–C in the saccharide structure. The strong bands at 1626 and 1418 cm^{-1} correspond to the asymmetric and symmetric stretching of carboxyl groups, respectively [22]. As for Co@AHs, there are clear shifts in the asymmetric vibrations of carboxyl groups from 1626 to 1619 cm^{-1}, and symmetric vibrations of these groups from 1418 to 1425 cm^{-1}, indicating some disorder in the biopolymer system [19,23]. Moreover, the peak at 676 cm^{-1} corresponding to metal–ligand interaction disappears in the Co@AHs due to the reduction of Co^{2+} to Co.

The elemental composition and electronic structure of the Co@AHs were investigated by X-ray photoelectron spectroscopy (XPS). Fig. 3 shows the XPS survey spectrum and high-resolution XPS spectra of the Co@AHs. The XPS survey spectrum (Fig. 3a) demonstrates that C, O, Ca, Na, and Co elements existed in the Co@AHs sample, where C, O, and Na elements could be associated with alginate. Fig. 3b shows high-resolution XPS spectrum of the C 1s, which can be deconvoluted into three surface components, corresponding to non-oxygenated ring carbon (C–C) at binding energy of 284.8 eV [24], oxygen-containing carbon (C–OH and O–C–O) at binding energy of 286.1 eV [24,25], as well as carboxyl carbon (O–C=O) at binding energy of 289.4 eV [26,27]. The high-resolution XPS spectrum of the O 1s can be fitted by two peaks at binding energies of around 532.2 and 531.2 eV (Fig. 3c), which are attributed to oxygen making single bonds carbon (C–OH and O–C–O) and O–C=O, respectively [24]. As shown in Fig. 3d, the binding energies of Co $2p_{3/2}$ and Co $2p_{1/2}$ are observed at 781.3 and 796.7 eV, respectively, which are the characteristic of surface Co(II) species [28,29]. The shakeup satellite peaks at approximately 5 eV above their main peaks can be further evidence of surface Co(II) species [30]. The detectable Co(II) species can be ascribed to the surface Co combined with oxygen of atmosphere during the catalyst preparation and storage process [31,32], which is similar to the other cobalt-based catalysts [33–35]. Additionally, other peaks at the low binding energies of 779.8 and 795.0 eV correspond to the Co $2p_{3/2}$ and Co $2p_{1/2}$ of metallic Co(0) [36,37]. As shown in Fig. 3e, the binding energies of Ca $2p_{1/2}$ and Ca $2p_{3/2}$ are observed at 350.6 and 347.0 eV, respectively, which are characteristic of Ca^{2+} [38,39], indicating the divalent calcium ion existed in the Co@AHs.

Fig. 4a shows a typical digital photograph of the Ca^{2+}/Co^{2+}-AHs beads in the swollen state. They are nearly spherical in shape and uniform in size. The average diameter of Ca^{2+}/Co^{2+}-AHs beads is ca. 2.5 mm. In addition, unlike the white Ca^{2+}-AHs beads (inset in Fig. 4a), the Ca^{2+}/Co^{2+}-AHs beads present light red in color (in the web version) due to the presence of Co^{2+} species. The microstructure of the Ca^{2+}/Co^{2+}-AHs beads was further observed by scanning electron microscopy (SEM). A general SEM image (inset in Fig. 4b) of the dried Ca^{2+}/Co^{2+}-AHs beads reveals their characteristic egg-like morphology. The magnified images (Fig. 4b, c) show that the beads have coarse surface with some visible wrinkles. After *in situ* chemical reduction by $NaBH_4$, the black Co@AHs beads were formed (Fig. 4d). Different from the wrinkled surface of Ca^{2+}/Co^{2+}-AHs beads, the Co@AHs beads show some cracks and macropores on their surface (Fig. 4e). The magnified SEM image shown in Fig. 4f

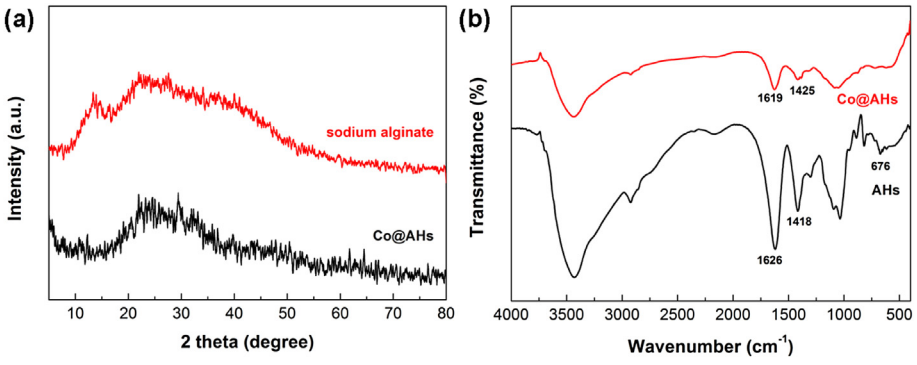

Fig. 2. XRD pattern (a) and FTIR spectra (b) of the Co@AHs.

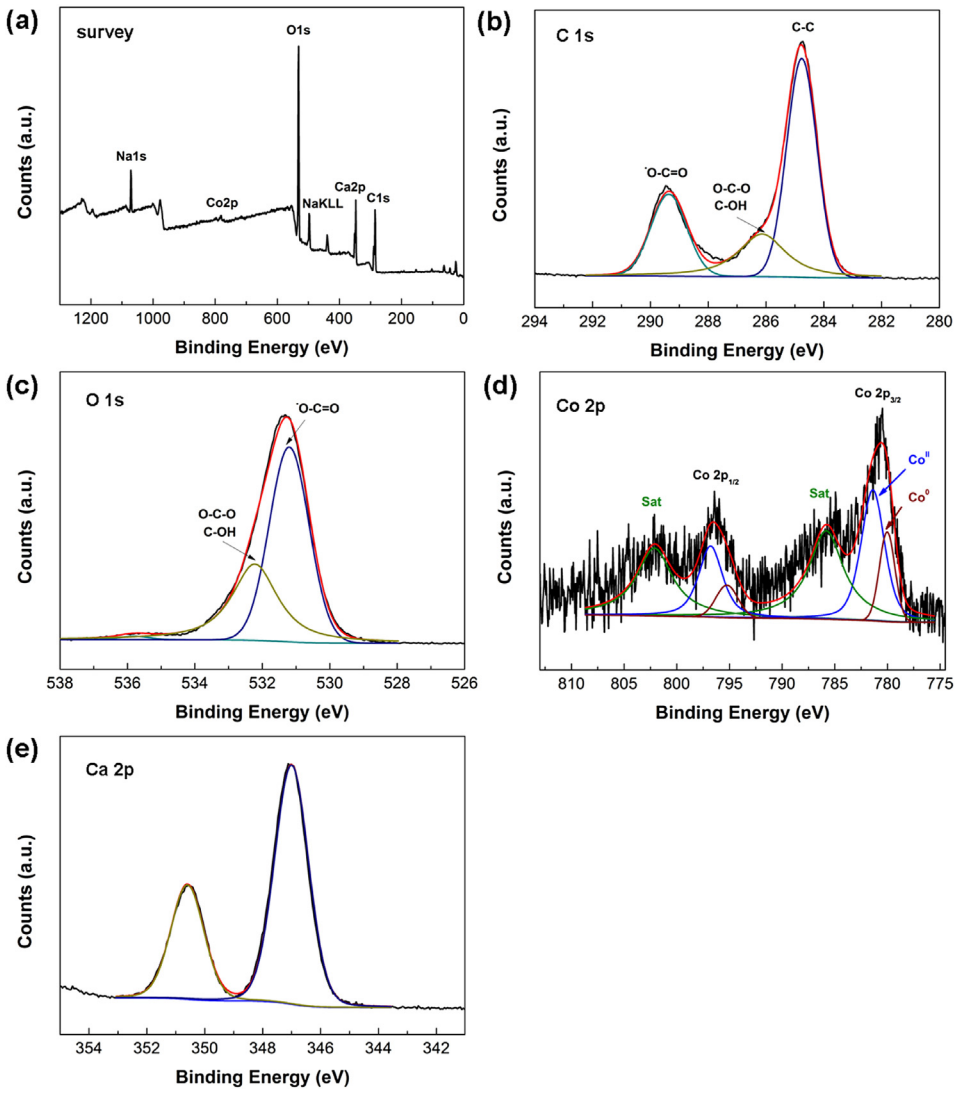

Fig. 3. XPS spectra of the Co@AHs: (a) survey, (b) C 1s, (c) O 1s, (d) Co 2p and (e) Ca 2p.

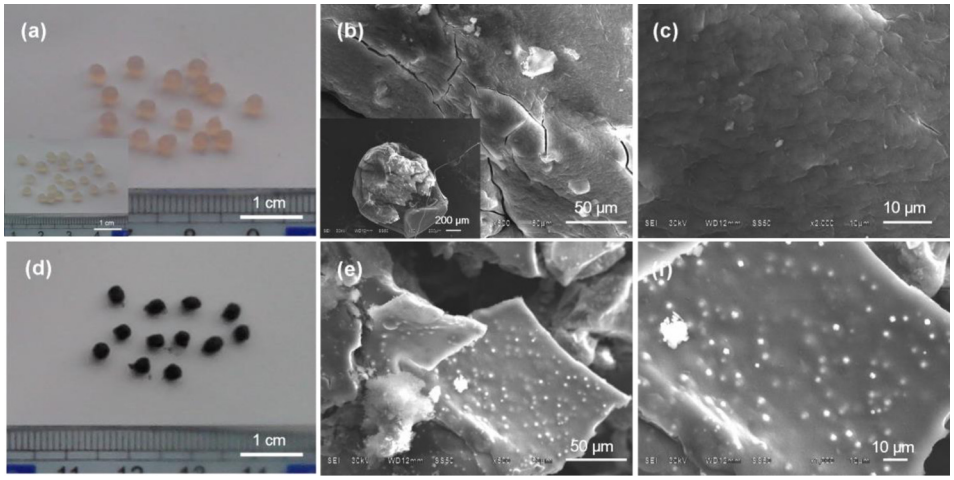

Fig. 4. Digital photograph (a) and SEM images (b, c) of Ca^{2+}/Co^{2+}-AHs beads. Digital photograph (d) and SEM images (e, f) of Co@AHs beads. Inset in figures (a) and (b) is the digital photograph of Ca^{2+}-AHs beads and low magnification SEM image of Ca^{2+}/Co^{2+}-AHs beads, respectively.

further demonstrates that lots of fine Co particles are well-embedded into the alginate polymer matrix. The compositional analysis of the Co@AHs was further determined by energy-dispersive X-ray spectroscopy (EDS) measurements (Fig. 5), which reveals the presence of Ca, Co, Na, C and O elements. The corresponding EDS mappings verify that these elements are homogeneously distributed in the Co@AHs.

The catalytic activity on the hydrolysis of aqueous $NaBH_4$ solution for hydrogen generation was tested for the Co@AHs catalysts. This hydrolysis reaction can be briefly expressed as: $NaBH_4 + 2H_2O \rightarrow NaBO_2 + 4H_2$. Fig. 6 shows the amount of H_2 generated as a function of reaction time from an alkaline $NaBH_4$ solution catalyzed by different catalysts. The bare Ca^{2+}-AHs shows no detectable catalytic activity towards the hydrolysis of $NaBH_4$. We thus believe that the catalytic contribution of Ca^{2+}-AHs in this study was negligible. In contrast, the remarkable H_2 generation was observed in the presence of the Co@AHs as catalysts, indicating their high catalytic activity to $NaBH_4$ hydrolysis. Such significantly improved catalytic activity is believed to arise from the appearance of metallic cobalt particles in the Co@AHs. As aforementioned, metallic cobalt particles are well-embedded into the alginate polymer matrix. Due to the appearance of various functional groups, cobalt particles could be stabilized by the alginate polymer. Therefore, the excellent catalytic activity is achieved by metallic cobalt particles protected by alginate polymer. Noticeably, the accumulative volume of H_2 generated during $NaBH_4$ hydrolysis increased linearly as the reaction time, implying the hydrolysis reaction follows the pseudo-zero order kinetics [40]. Fig. 6 also depicts the catalytic activity of the Co@AHs with different dosage. It is evident that the amounts of H_2 generation for the $NaBH_4$ hydrolysis increased with the increasing the catalyst dosage under the same conditions. When the dosage of the Co@AHs changed from 10 beads to 30 beads, the average H_2 generation rate raised gradually

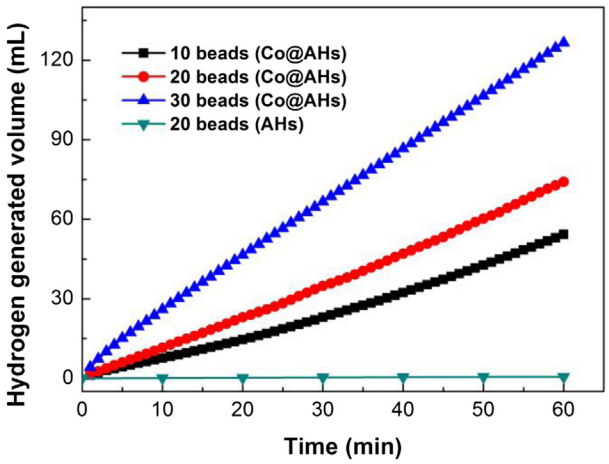

Fig. 6. Catalytic activity of the Co@AHs and Ca^{2+}-AHs on the hydrogen generation by hydrolysis of $NaBH_4$ solution (10 mL, 5 wt%) containing 5 wt% NaOH at 30 °C.

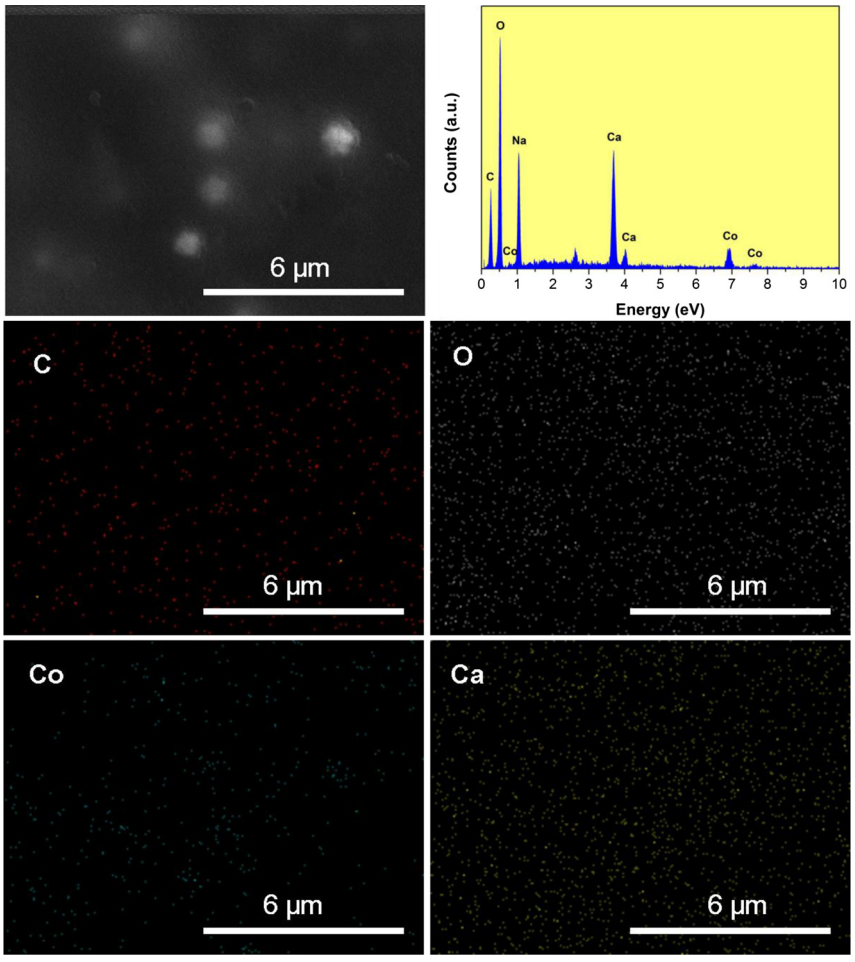

Fig. 5. SEM–EDS spectrum and compositional mapping images of the Co@AHs beads.

from 0.888 to 2.03 mL min^{-1}. Obviously, the H_2 generation rate could be rationally controlled by adjusting the catalyst dosage used in the hydrolysis reaction.

The alkaline (such as NaOH) stabilized $NaBH_4$ solution is generally employed as feed stock for H_2 generation because introduction of NaOH could efficiently inhibit the self-hydrolysis of $NaBH_4$ [3,40]. The effect of the NaOH concentration on H_2 generation rate was investigated by hydrolysis of 10 mL 5 wt% $NaBH_4$ solution at 30 °C with 20 beads of the Co@AHs. Fig. 7 shows the catalytic activity of the Co@AHs in the presence of different NaOH concentrations. It is clear that increasing the NaOH concentration from 1 to 5 wt% could enhance the average H_2 generation rates from 0.943 to 1.223 mL min^{-1}, indicating that NaOH is favorable for the $NaBH_4$ hydrolysis for H_2 generation over the Co@AHs. A similar observations were also reported in the catalytic systems of Co-ZIF-9 [41], p(AAGA)-Co [42], Co(II)–Cu(II) based complex catalyst [43], and attapulgite clay-supported Co–B [44]. However, it should be noted that the catalytic activity is only 1.3-fold increase when the NaOH concentration increases from 1 to 5 wt%, indicating the catalytic activity of the Co@AHs is weakly dependent on the concentration of NaOH.

Considering that $NaBH_4$ is the hydrogen source in the hydrolysis reaction, its concentration is crucial for kinetics of the catalytic reaction. The effect of the $NaBH_4$ concentration on H_2 generation rate was investigated by hydrolysis of 10 mL 5 wt% $NaBH_4$ solution at 30 °C with 20 beads of the Co@AHs. Fig. 8 shows the catalytic activity of the Co@AHs in the presence of different $NaBH_4$ concentrations. The H_2 generation rate increases significantly when the concentration of $NaBH_4$ increases from 1 wt% to 2 wt%, but reduces remarkably when the $NaBH_4$ concentration further increases to 10 wt%. This phenomenon is attributed to the fact that the viscosity of reaction medium could increase with an excessive increase in $NaBH_4$ concentration, leading to reducing the hydrolysis rate of $NaBH_4$. Moreover, the hydrolyzed product of $NaBH_4$ is mainly $NaBO_2$, which has a lower solubility than that of $NaBH_4$. Apparently, the formation of $NaBO_2$ could interrupt mass transfer between $NaBH_4$ molecules and catalysts, thus decreasing the activity of catalysts.

To investigate the effect of temperature on the H_2 generation rate, $NaBH_4$ hydrolysis reaction was also performed at various temperatures. Fig. 9 shows the catalytic activity of the Co@AHs at different temperatures. The H_2 generation rates increase

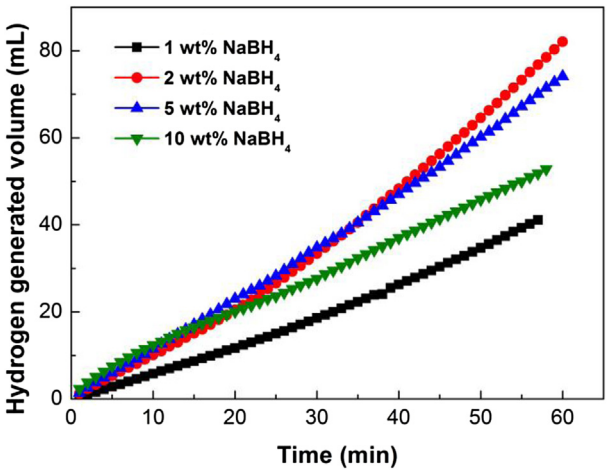

Fig. 8. Catalytic activity of the Co@AHs (20 beads) on the hydrogen generation by hydrolysis of different concentrations of $NaBH_4$ solution (10 mL) containing 5 wt% NaOH at 30 °C.

dramatically with the increase in temperature. From the Arrhenius plots of ln k vs. the reciprocal absolute temperature ($1/T$) for the Co@AHs (inset in Fig. 9), the apparent activation energy (E_a) is calculated to be 55.6 kJ mol^{-1}, which is comparable to the reported E_a values for the hydrolysis reaction of $NaBH_4$ catalyzed by CoO nanocrystals (58.5 kJ mol^{-1}) [45], Ni–Ni_3B (55.81 kJ mol^{-1}) [46], CoB/CeO_2 (55.3 kJ mol^{-1}) [47] and Co–B/C (57.8 kJ mol^{-1}) [48], and is lower than that of anisotropy Co–B catalyst (68.87 kJ mol^{-1}) [49], Co–P catalyst (60.2 kJ mol^{-1}) [50], Co–La–Zr–B (60.06 kJ mol^{-1}) [51], and Ni–Co–B (62.00 kJ mol^{-1}) [52]. The remarkable activity of Co@AHs could be ascribed to the unique porous surface structures (Fig. 4), which are favorable for the exposure of more surface active sites and facile mass transportation for the heterogenous hydrolysis of $NaBH_4$. In addition, the cobalt particles were well-immobilized on the biopolymer matrix that could prevent them from aggregation to maintain high stability.

After the catalytic reaction, the Co@AHs catalysts can be easily separated by taking hydrogel beads out of the catalytic system due to its macroscopic nature (Fig. 4d). Such an easy separation is particularly attractive. Therefore, the recyclability of the Co@AHs was tested by performing the $NaBH_4$ hydrolysis in successive cycles. As shown in Fig. 10a, it is interesting that the H_2 generation rates

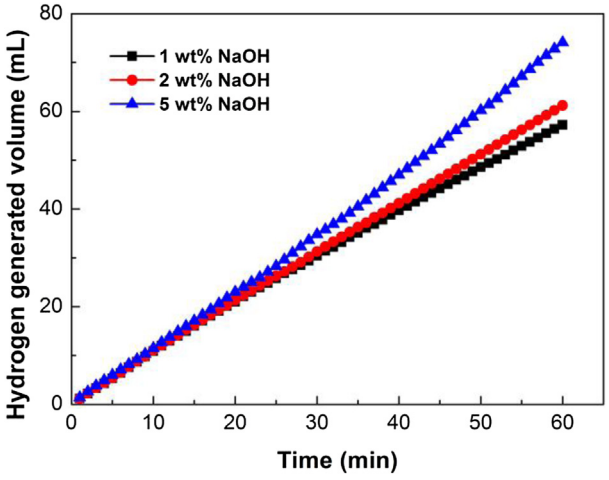

Fig. 7. Catalytic activity of the Co@AHs (20 beads) on the hydrogen generation by hydrolysis of $NaBH_4$ solution (10 mL, 5 wt%) containing different concentrations of NaOH at 30 °C.

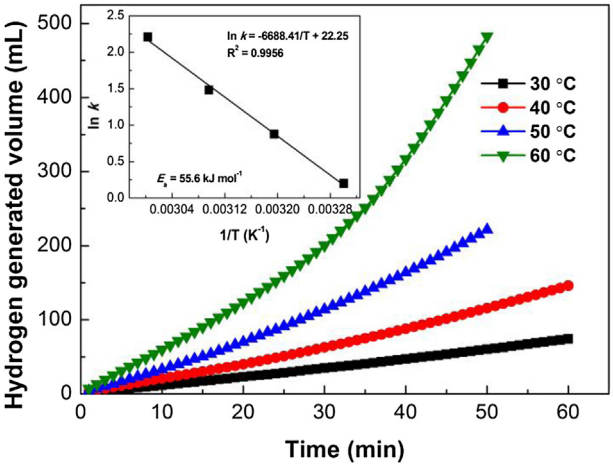

Fig. 9. Catalytic activity of the Co@AHs on the hydrogen generation by hydrolysis of $NaBH_4$ solution (10 mL, 5 wt%) containing 5 wt% NaOH at different temperatures.

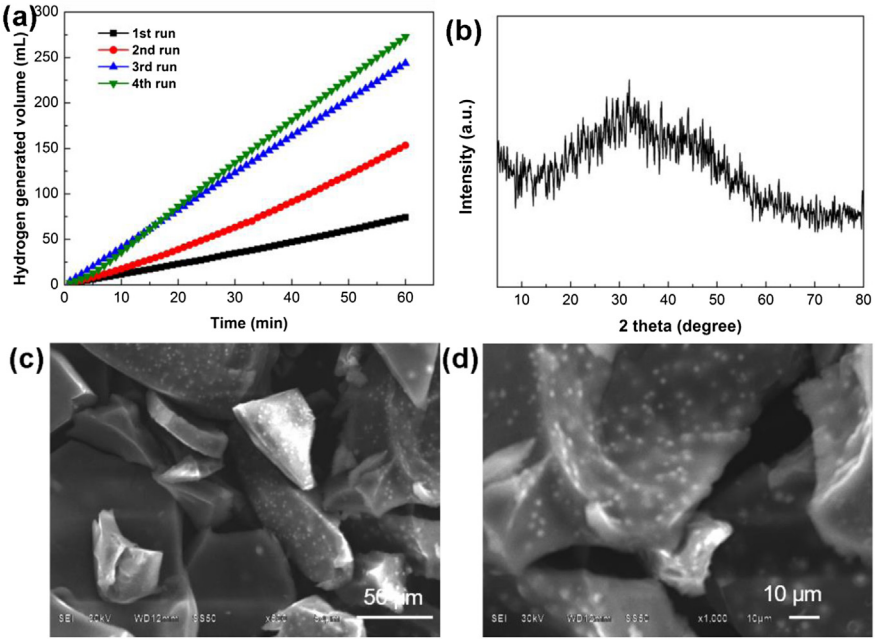

Fig. 10. (a) Reusability test of hydrogen generation from hydrolysis of $NaBH_4$ solution (10 mL, 5 wt%) containing 5 wt% NaOH catalyzed by the Co@AHs (20 beads) at 30 °C. (b) XRD pattern and (c, d) SEM images of the Co@AHs after catalytic reaction.

increase significantly for the Co@AHs from the first run to third run and remain at the same level in the following runs. In the fourth cycle, the average H_2 rate reaches up to 4.725 mL min^{-1}, which is 3.86 times that of the first run. This unique recyclability is distinct from that of the cobalt-supported catalysts [7,53,54]. As aforementioned, the alginate is a typical biopolymer with abundant oxygen-containing functional groups (Fig. 1). Thus, it would be active in our reaction medium. Accordingly, the wrinkled surface of the AHs beads is cracked, resulting in the formation of macropore during the *in situ* synthesis process. After four cycles of the catalytic reactions, this change in surface structure becomes more clear (Fig. 10c), which may be crucial for the performance of the observed recyclability. Actually, the large amounts of active Co species are enveloped by alginate polymers during the *in situ* synthesis process. So the cracked and porous surface structure is beneficial for the diffusion of reactants into the inner space of beads, significantly improving the contact between reactants and active surface sites, thus increasing the H_2 generation rate. In addition, the XRD patterns (Fig. 10b) and SEM image (Fig. 10d) of the Co@AHs after fourth cycle presents similar crystallinity and morphology to that of the *in situ* synthesized Co@AHs. These results indicate clearly that the Co@AHs catalysts possess excellent durability and recyclability for catalytic reactions of $NaBH_4$ hydrolysis. Moreover, the increased production in hydrogen after successive runs coupled with the change in morphology seems to suggest that the efficiency of this catalyst may be due to increased disorder in the system thus causing a larger surface area. It would appear that the initial reduction in $NaBH_4$ also causes this disorder (Fig. 4), which could be an additional reason why the Co@AHs catalyst works better in the cycled reaction.

4. Conclusions

In summary, the Co@AHs catalysts have been designed and fabricated by an *in situ* chemical reduction method for the first time. In the synthesis process, cobalt ions serve as a cross-linker of polysaccharide chains to induce alginate gelation, ensuring the uniform distribution of metallic Co in AHs. The Co@AHs catalysts exhibit an excellent catalytic performance for the hydrogen generation from $NaBH_4$ hydrolysis. More interestingly, the Co@AHs catalyst can be easily separated after catalytic reaction and readily recycled over four successive cycles of the reactions. Since the eco-friendly and inexpensive Co@AHs are catalytically effective with superior recyclability, it is reasonable to believe that our Co@AHs will be a promising candidate for the substitution of noble metal catalysts in the hydrogen generation from the hydrolysis of borohydrides.

Acknowledgments

This work was supported by the National Natural Science Foundation of China (21103141 and 21207108), the Sichuan Youth Science and Technology Foundation (2013JQ0012), the Applied Basic Research Program of Sichuan Provincial Science and Technology Department (2011JYZ019) and the Research Foundation of CWNU (12B018).

References

[1] S. Zinoviev, F. Muller-Langer, P. Das, N. Bertero, P. Fornasiero, M. Kaltschmitt, G. Centi, S. Miertus, ChemSusChem 3 (2010) 1106–1133.
[2] M. Li, D.A. Cullen, K. Sasaki, N.S. Marinkovic, K. More, R.R. Adzic, J. Am. Chem. Soc. 135 (2013) 132–141.
[3] R. Retnamma, A.Q. Novais, C.M. Rangel, Int. J. Hydrogen Energy 36 (2011) 9772–9790.
[4] U.B. Demirci, P. Miele, Phys. Chem. Chem. Phys. 12 (2010) 14651–14665.
[5] L. Chong, J. Zou, X. Zeng, W. Ding, J. Mater. Chem. A 1 (2013) 3983–3991.
[6] M. Yadav, Q. Xu, Energy Environ. Sci. 5 (2012) 9698–9725.
[7] F. Qiu, L. Li, G. Liu, Y. Wang, Y. Wang, C. An, Y. Xu, C. Xu, Y. Wang, L. Jiao, H. Yuan, Int. J. Hydrogen Energy 38 (2013) 3241–3249.
[8] X. Yang, F. Cheng, J. Liang, Z. Tao, J. Chen, Int. J. Hydrogen Energy 36 (2011) 1984–1990.
[9] J.-M. Yan, Z.-L. Wang, H.-L. Wang, Q. Jiang, J. Mater. Chem. 22 (2012) 10990–10993.
[10] Z.-H. Lu, H.-L. Jiang, M. Yadav, K. Aranishi, Q. Xu, J. Mater. Chem. 22 (2012) 5065–5071.
[11] T. Umegaki, J.-M. Yan, X.-B. Zhang, H. Shioyama, N. Kuriyama, Q. Xu, J. Power Sources 195 (2010) 8209–8214.

[12] M. Zahmakıran, T. Ayvali, S. Akbayrak, S. Caliskan, D. Celik, S. Ozkar, Catal. Today 170 (2011) 76–84.
[13] X. Wang, D. Liu, S. Song, H. Zhang, Chem. Commun. 48 (2012) 10207–10209.
[14] S.B. Kalidindi, U. Sanyal, B.R. Jagirdar, Phys. Chem. Chem. Phys. 10 (2008) 5870–5874.
[15] S. Sagbas, N. Sahiner, Int. J. Hydrogen Energy 37 (2012) 18944–18951.
[16] F. Seven, N. Sahiner, Int. J. Hydrogen Energy 38 (2013) 777–784.
[17] L. Ai, H. Yue, J. Jiang, J. Mater. Chem. 22 (2012) 23447–23453.
[18] L. Ai, J. Jiang, Bioresour. Technol. 132 (2013) 374–377.
[19] Y. Dong, W. Dong, Y. Cao, Z. Han, Z. Ding, Catal. Today 175 (2011) 346–355.
[20] C. Chang, B. Duan, L. Zhang, Polymer 50 (2009) 5467–5473.
[21] F. Chen, M. Tian, D. Zhang, J. Wang, Q. Wang, X. Yu, X. Zhang, C. Wan, Mater. Sci. Eng. C 32 (2012) 310–320.
[22] J.S. Yang, B. Jiang, W. He, Y.M. Xia, Carbohydr. Polym. 87 (2012) 1503–1506.
[23] L. Fuks, D. Filipiuk, M. Majdan, J. Mol. Struct. 792–793 (2006) 104–109.
[24] S.K. Tama, J. Dusseault, S. Polizu, M. Menard, J.-P. Halle, L.H. Yahia, Biomaterials 26 (2005) 6950–6961.
[25] S. Hu, R. Tian, L. Wu, Q. Zhao, J. Yang, J. Liu, S. Cao, Chem. Asian J. 8 (2013) 1035–1041.
[26] J. Mu, C. Shao, Z. Guo, Z. Zhang, M. Zhang, P. Zhang, B. Chen, Y. Liu, ACS Appl. Mater. Interfaces 3 (2011) 590–596.
[27] H. Seema, K.C. Kemp, V. Chandra, K.S. Kim, Nanotechnology 23 (2012) 355705.
[28] D. Xu, P. Lu, P. Dai, H. Wang, S. Ji, J. Phys. Chem. C 116 (2012) 3405–3413.
[29] Y. Yamada, K. Yano, Q. Xu, S. Fukuzumi, J. Phys. Chem. C 114 (2010) 16456–16462.
[30] S. Bennici, H. Yu, E. Obeid, A. Auroux, Int. J. Hydrogen Energy 36 (2011) 7431–7442.
[31] M. Rakap, S. Ozkar, Catal. Today 183 (2012) 17–25.
[32] M. Rakap, S. Ozkar, Appl. Catal. B Environ. 91 (2009) 21–29.
[33] J. Delmas, L. Laversenne, I. Rougeaux, P. Capron, A. Garron, S. Bennici, D. Swierczynski, A. Auroux, Int. J. Hydrogen Energy 36 (2011) 2145–2153.
[34] Y. Zhao, Z. Ning, J. Tian, H. Wang, X. Liang, S. Nie, Y. Yu, X. Li, J. Power Sources 207 (2012) 120–126.
[35] J. Andrieuxa, D. Swierczynski, L. Laversenne, A. Garron, S. Bennici, C. Goutaudier, P. Miele, A. Auroux, B. Bonnetot, Int. J. Hydrogen Energy 34 (2009) 938–951.
[36] M. Zhang, Y. Jin, Q. Wen, C. Chen, M. Jia, Appl. Surf. Sci. 277 (2013) 25–29.
[37] R. Riva, H. Miessner, R. Vitali, G.D. Piero, Appl. Catal. A 196 (2000) 111–123.
[38] U.G. Akpan, B.H. Hameed, J. Colloid Interface Sci. 357 (2011) 168–178.
[39] P. Zhang, G. Qian, Z.P. Xu, H. Shi, X. Ruan, J. Yang, R.L. Frost, J. Colloid Interface Sci. 367 (2012) 264–271.
[40] H. Li, J. Liao, X. Zhang, W. Liao, L. Wen, J. Yang, H. Wang, R. Wang, J. Power Sources 239 (2013) 277–283.
[41] Q. Li, H. Kim, Fuel Process. Technol. 100 (2012) 43–48.
[42] N. Sahiner, S. Butun, T. Turhan, Chem. Eng. Sci. 82 (2012) 114–120.
[43] D. Kilinc, C. Saka, O. Sahin, J. Power Sources 217 (2012) 256–261.
[44] H. Tian, Q. Guo, D. Xu, J. Power Sources 195 (2010) 2136–2142.
[45] A. Lu, Y. Chen, J. Jin, G.-H. Yue, D.-L. Peng, J. Power Sources 220 (2012) 391–398.
[46] A.A. Vernekar, S.T. Bugde, S. Tilve, Int. J. Hydrogen Energy 37 (2012) 327–334.
[47] Y.-C. Lu, M.-S. Chen, Y.-W. Chen, Int. J. Hydrogen Energy 37 (2012) 4254–4258.
[48] J. Zhao, H. Ma, J. Chen, Int. J. Hydrogen Energy 32 (2007) 4711–4716.
[49] S.U. Jeong, R.K. Kim, E.A. Cho, H.J. Kim, S.W. Nam, I.H. Oh, S.A. Hong, S.H. Kim, J. Power Sources 144 (2005) 129–134.
[50] K.S. Eom, K.W. Cho, H.S. Kwon, J. Power Sources 180 (2008) 484–490.
[51] M.H. Loghmani, A.F. Shojaei, J. Alloys Compd. 580 (2013) 61–66.
[52] J.C. Ingersoll, N. Mani, J.C. Thenmozhiyal, A. Muthaiah, J. Power Sources 173 (2007) 450–457.
[53] F. Qiu, L. Li, G. Liu, Y. Wang, C. An, C. Xu, Y. Xu, Y. Wang, L. Jiao, H. Yuan, Int. J. Hydrogen Energy 38 (2013) 7291–7297.
[54] D. Sun, V. Mazumder, O. Metin, S. Sun, ACS Catal. 2 (2012) 1290–1295.